Distorted Bounding Surface of Clay with Consideration of the Effect of Temperature on Shearing Response

Sang Inn Woo
Department of Civil and Environmental Engineering, Hannam University, Daedeok-gu, Daejeon, South Korea
Chan-Young Yune
Department of Civil Engineering, Gangneung-Wonju National University, Gangneung-si, Gangwon-do, South Korea

ABSTRACT
The present paper proposes a bounding surface to describe shearing response of clay depending on temperature. As temperature increases, normal consolidation line moves down in the plane of void ratio and mean effective stress. The critical state line, however, does not shifts as much as the normal consolidation line upon temperature change. Therefore, the critical state mean effective stress moves to the pre-consolidation pressure as temperature increases. To naturally capture this, the proposed bounding surface consists of two parts divided at the critical state mean effective stress. The bounding surface was calibrated for the soft Bangkok clay. Elemental simulations from the proposed model showed the model performance to capture the critical state (which is destination of clay upon shearing) without complex hardening and evolution rules compared to the experimental data.

RÉSUMÉ
Le présent article propose une surface limite pour décrire la réponse au cisaillement de l'argile en fonction de la température. À mesure que la température augmente, la ligne de consolidation normale descend dans le plan du taux de vide et de la contrainte effective moyenne. Cependant, la ligne d'état critique ne se déplace pas autant que la ligne de consolidation normale lors d'un changement de température. Par conséquent, la contrainte effective moyenne de l'état critique se déplace vers la pression de pré-consolidation à mesure que la température augmente. Pour capter naturellement cela, la surface de délimitation proposée est constituée de deux parties divisées à l'état critique, la contrainte effective moyenne. La surface de délimitation a été calibrée pour l'argile molle de Bangkok. Les simulations élémentaires du modèle proposé ont montré que le modèle permettait de capturer l'état critique (destination de l'argile lors du cisaillement) sans règles de durcissement et d'évolution complexes par rapport aux données expérimentales.

1 INTRODUCTION

The consolidation and shearing responses of a clay depends on temperature (Plum and Esrig 1969, Graham et al. 2001, Sultan et al. 2002, Neaupane et al. 2005, Abuel-Naga et al. 2007, Hamidi et al. 2014, Brochard et al. 2017). Previous studies on the consolidation behavior of clay upon temperature (Plum and Esrig 1969, Graham et al. 2001, Sultan et al. 2002, Neaupane et al. 2005, Abuel-Naga et al. 2007, Brochard et al. 2017) have shown that the location of normal consolidation line (NCL) depends on temperature in the plane of void ratio e and mean effective stress p'; it shifts downwards under the higher temperature. This implies that clay contracts (or pore water drains) under a fixed p' when temperature increases; thus, at the same void ratio e, the pre-consolidation pressure p'_c of normally consolidated (NC) clay is smaller at the higher temperature and with the identical p'_c, the NC clay has lower e at the higher temperature.

For shearing responses of clay, Hamidi et al. (2014) proposed that the critical state surface (CSS) in the stress space (e.g., the p'-q plane) can be affected by temperature while Graham et al. (2001) and Abuel-Naga et al. (2007) reported that there is no meaningful dependency of the CSS on temperature. For the critical state line (CSL) in the plane of void ratio e and mean effective stress p', Abuel-Naga et al. (2007) did not found meaningful dependency of CSL on temperature; however, Graham et al. (2001) reported that CSL moves down slightly (not as much as normal consolidation line (NCL) does) as temperature increases. Based on these previous researches on the consolidation behavior and shearing responses of clay, the ratio between the critical state mean effective stress p'_{cs} and pre-consolidation pressure p'_c changes when temperature changes.

To describe this dependency numerically, the Modified Cam Clay (MCC) model has been adopted by many researchers (Graham et al. 2001, Hamidi et al. 2014, Wang et al. 2016). In the yield (or bounding) surface of the MCC model, the ratio p'_{cs}/p'_c is fixed as 0.5 as the surface is an ellipse in the p'-q plane; thus, with the original MCC yield surface, complex flow, hardening, and evolution rules are required to realistically describe shearing responses under different temperature.

The aim of this study is to propose a new MCC type distorted bounding surface (or yield surface) to capture temperature dependency of the shearing response of clay in a simple way. The bounding surface has two parts

which join at (p', $M_c p'_{cs}$) (where M_c is the critical state stress ratio (= q_{cs}/p'_{cs})) which is the apex of the bounding surface.

The present paper suggests the constitutive modeling on which CSL and the present bounding surface is dependent on temperature change in Section 2. Section 3 describes the calibration of the bounding surface for the soft Bangkok clay. Section 4 shows the model performance in simulating the experiments of the soft Bangkok clay. Section 5 summarizes the contributions of the present paper and possible future researches.

As this study focuses on the mechanical response of clay under the triaxial conditions, the constitutive model is formulated based on stress invariants p' and q and strain invariants ε_{vol} and ε_q. In the indicial notation, they are defined as

$$p' = \frac{1}{3}\sigma'_{kk},\ q = \sqrt{\frac{3}{2}s_{ij}s_{ij}} \quad [1]$$

$$\varepsilon_{vol} = \varepsilon_{kk},\ \varepsilon_q = \sqrt{\frac{2}{3}e_{ij}e_{ij}} \quad [2]$$

where σ'_{ij} is effective stress (= $\sigma_{ij} - u\delta_{ij}$), σ_{ij} is total stress, u is porewater pressure, s_{ij} is deviatoric stress (= $\sigma'_{ij} - p'\delta_{ij}$), ε_{ij} is strain, and e_{ij} is deviatoric strain (= $\varepsilon_{ij} - (1/3)\varepsilon_{kk}\delta_{ij}$).

2 CONSTITUTIVE MODELING

2.1 Consolidation Behavior

When p' and e are control variables, the mathematical expressions for the normal consolidation line (NCL) are

$$e_{NC} = N - \lambda \ln\left(\frac{p'}{p_A}\right) \quad [3]$$

$$p'_c = p_A \exp\left[\frac{N-e}{\lambda}\right] \quad [4]$$

respectively, where e_{NC} is void ratio along the NCL, p_A is the reference pressure (≈ 100 kPa), N is e_{NC} when $p' = p_A$, λ is a material constant that represents the slope of NCL and p'_c is pre-consolidation pressure. According to the previous studies (Plum and Esrig 1969, Graham et al. 2001, Sultan et al. 2002, Neaupane et al. 2005, Abuel-Naga et al. 2007), as temperature increases, NCL moves down with a fixed slope in e'-lnp' plane; this implies that N is a function of temperature. In this study, to describe the dependency of N on temperature, N is set as in

$$N = N(T) = N_{ref} - \alpha\left(T - T_{ref}\right) \quad [5]$$

where T_{ref} is reference temperature, N_{ref} is N at T_{ref}, and α is a positive material constant. The swelling (or recompression) line is

$$e_{OC} = e_{NC,c} + \kappa \ln\left(\frac{p'}{p'_c}\right) \quad [6]$$

where e_{OC} is void ratio along the swelling line, p'_c is pre-consolidation pressure, and $e_{NC,c}$ is void ratio when $p' = p'_c$ on NCL.

2.2 Strain Decomposition & Elastic Behavior

This study assumes that a strain increment consists of elastic and plastic strain increments:

$$\mathrm{d}\varepsilon_{vol} = \mathrm{d}\varepsilon^e_{vol} + \mathrm{d}\varepsilon^p_{vol},\ \mathrm{d}\varepsilon_q = \mathrm{d}\varepsilon^e_q + \mathrm{d}\varepsilon^p_q \quad [7]$$

where superscripts e and p represent elastic and plastic strains, respectively. From the elasticity theory, relationships between stress increment invariants (dp' and dq) and elastic strain increment invariants (dε^e_{vol} and dε^e_q) are:

$$\mathrm{d}p' = K\mathrm{d}\varepsilon^e_{vol},\ \mathrm{d}q = 3G\mathrm{d}\varepsilon^e_q \quad [8]$$

where K and G are the bulk and shear moduli, respectively. The clay is typically assumed to be elastic along the swelling (or recompression) line; thus, in this study, the bulk modulus is related to κ according to:

$$K = \frac{(1+e)\,p'}{\kappa} \quad [9]$$

This study set the shear modulus of clay as a function of the bulk modulus and Poisson's ratio ν.

$$G = \frac{3K(1-2\nu)}{2(1+\nu)} \quad [10]$$

2.3 Critical State

For clays, the critical state is quantified using the critical state surface (CSS) in the stress space (e.g., the p'-q plane) and the critical state line (CSL) in the space of e and p'. In the p'-q space, a linear function has been used for the CSS:

$$q = M_c p' \quad [11]$$

where M_c is the critical state stress ratio that represents the slope of CSS. Hamidi et al. (2014) reported that the CSS slightly depends on the temperature while Graham et al. (2001) and Abuel-Naga et al. (2007) found no meaningful dependency of the CSS on temperature. In the present model, the CSS is assumed to be independent of temperature following Graham et al. (2001) and Abuel-Naga et al. (2007).

Graham et al. (2001) and Abuel-Naga et al. (2007) reported that the CSL has been assumed to be parallel to NCL; thus, when p' and e are control variables, CSL can be mathematically written as:

$$e_{cs} = \Gamma - \lambda \ln\left(\frac{p'}{p_A}\right) \quad [12]$$

$$p'_{cs} = p_A \exp\left[\frac{\Gamma - e}{\lambda}\right] \quad [13]$$

respectively, where e_{CS} is void ratio along CSL. Although Abuel-Naga et al. (2007) stated that there is no meaningful dependency of CSL on temperature, Graham et al. (2001) reported that CSL (as well as NCL) moves down as temperature increases. In this study, following Graham et al. (2001), the location of CSL depending on temperature is determined using

$$\Gamma = \Gamma(T) = \Gamma_{ref} - \beta\left(T - T_{ref}\right) \quad [14]$$

where Γ_{ref} is Γ when $T = T_{ref}$ and β is a positive material constant.

2.4 Bounding Surface

Construction of an MCC type bounding surface (which is an ellipse in the p'-q plane) requires two points: its apex and right end along the p' axis. From the consolidation theory, the right end of the bounding surface is where plastic volumetric strain starts to generate; thus, this point corresponds to the pre-consolidation pressure p'_c. According to the associated flow rule, upon shearing, stress paths move to and are stabilized at the apex of the bounding surface; thus, the apex of the ellipse is related to the critical state and corresponds to (p'_{cs}, $M_c p'_{cs}$). In the original MCC model, as it uses an ellipse, the p' at the apex is always half of the right end of the ellipse; without hardening and evolution rules, it enforces $p'_{cs} = 1/2 p'_c$, which is not always true for clay; thus, MCC models have frequently requires complex flow, hardening, and evolution rules to describe the realistic mechanical responses of clay.

For thermal effect on shearing responses of clay, Abuel-Naga et al. (2007) found no meaningful dependency of CSL on temperature. Graham et al. (2001) reported that CSL (as well as NCL) moves down as temperature increases; however, CSL doesn't shift as much as NCL does. As a result, the ratio p'_{cs}/p'_c changes as temperature changes; thus, even more sophisticated hardening (and evolution) rules (Graham et al. 2001, Hamidi et al. 2014, Wang et al. 2016) were required to describe the thermal effect using the ellipse shaped MCC yield (or bounding) surface.

To simply describe the thermomechanical responses of clay, this study builds up a distorted MCC type bounding surface. Figure 1 schematically illustrates a bounding surface proposed in this study in the p'-q plane. When $p' \le p'_{cs}$, the bounding surface is left half of an eclipse of which right end is ($2p'_{cs}$, 0) and apex is (p'_{cs}, Mp'_{cs}). Mathematically, it can be expressed by

$$f = \frac{\left(p' - p'_{cs}\right)^2}{p'^2_{cs}} + \frac{q^2}{M^2 p'^2_{cs}} - 1 = 0 \quad [15]$$

When $p' > p'_{cs}$, the bounding surface is right half of an eclipse of which right end is ($2p'_c$, 0) and apex is (p'_{cs}, Mp'_{cs}). Mathematically, it can be expressed by

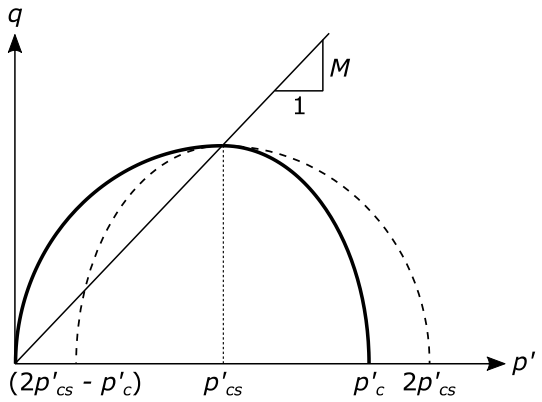

Figure 1. Bounding surface proposed in this study

$$f = \frac{\left(p' - p'_{cs}\right)^2}{\left(p'_c - p'_{cs}\right)^2} + \frac{q^2}{M^2 p'^2_{cs}} - 1 = 0 \quad [16]$$

As shown as Figure 1, using half parts from two ellipses for a bounding surface, there is no constraint in the ratio between p'_{cs} and p'_c. The derivatives of the bounding surface with respect to the stress invariants p' and q are

$$\frac{\partial f}{\partial p'} = \frac{2\left(p' - p'_{cs}\right)}{p'^2_{cs}}, \quad \frac{\partial f}{\partial q} = \frac{2q}{M^2 p'^2_{cs}} \qquad \text{if } p' \le p'_{cs} \quad [17]$$

$$\frac{\partial f}{\partial p'} = \frac{2\left(p' - p'_{cs}\right)}{\left(p'_c - p'_{cs}\right)^2}, \quad \frac{\partial f}{\partial q} = \frac{2q}{M^2 p'^2_{cs}} \qquad \text{if } p' > p'_{cs} \quad [18]$$

2.5 Calculation of Plastic Multiplier

In the present model, the clay follows the associated flow rule; thus, the invariants of a plastic strain increment are written as:

$$\mathrm{d}\varepsilon_{vol}^{p} = \mathrm{d}\Lambda \frac{\partial f}{\partial p'},\ \mathrm{d}\varepsilon_{q}^{p} = \mathrm{d}\Lambda \frac{\partial f}{\partial q} \quad [19]$$

where dΛ is the plastic multiplier. The consistency condition states:

$$\begin{aligned} &\frac{\partial f}{\partial p'}\mathrm{d}p' + \frac{\partial f}{\partial q}\mathrm{d}q + \frac{\partial f}{\partial p_c'}\mathrm{d}p_c' + \frac{\partial f}{\partial p_{cs}'}\mathrm{d}p_{cs}' + \frac{\partial f}{\partial M}\mathrm{d}M \\ &= \frac{\partial f}{\partial p'}\mathrm{d}p' + \frac{\partial f}{\partial q}\mathrm{d}q - \mathrm{d}\Lambda H = 0 \end{aligned} \quad [20]$$

After organization of Equations [8], [19] and [20], the mathematical expression of the plastic multiplier is

$$\mathrm{d}\Lambda = \frac{K\mathrm{d}\varepsilon_{vol}\left(\frac{\partial f}{\partial p'}\right) + 3G\mathrm{d}\varepsilon_{q}\left(\frac{\partial f}{\partial q}\right)}{H + K\left(\frac{\partial f}{\partial p'}\right)^{2} + 3G\left(\frac{\partial f}{\partial q}\right)^{2}} \quad [21]$$

3 CALIBRATION

To calibrate the proposed bounding surface, the present study relies on the experimental data for soft Bangkok clay from Abuel-Naga et al. (2007) in which the reference temperature T_{ref} was set as 25°C. Figure 2 illustrates the calibration of N_{ref}, α, λ, and κ. In Figure 2, N is calibrated as 1.86 when $T = T_{ref}$ = 25 °C; thus, N_{ref} = 1.86. When T = 70 °C, NCL moves down and N decreases to 1.76. Using these values, α (= $(N_{25} - N_{70})/(N_{70} - N_{25})$ from Equation [5]) is calibrated as 2.22e−3 in this study. From the experimental data, the slope λ of NCL and slope κ of swelling lines sustain upon the temperature change; their values were calibrated as 0.405 and 0.055, respectively.

Figure 3 shows the calibration of CSS for the present model. In the figure, symbols represent the final destinations (which correspond to the critical state) of stress paths upon undrained triaxial compression tests. In this study, based on experimental results in Figure 3, the slope M_c of CSS is calibrated as 0.8, which was a proposed value in Abuel-Naga et al. (2007) for the soft Bangkok clay.

Figure 4 illustrates the calibration of Γ_{ref} and β which are parameters for the CSL. In Figure 4, Γ is calibrated as 1.66 when $T = T_{ref}$ = 25 °C; thus, Γ_{ref} = 1.66. When T = 70 °C, CSL slightly moves down and Γ reduces to 1.62. Using these values, β (= $(\Gamma_{25} - \Gamma_{70})/(\Gamma_{70} - \Gamma_{25})$ from Equation [14]) is calibrated as 8.89e−4 in this study. Additionally, the experimental data well agrees to the assumption that the slope CSL is identical to the slope λ of NCL. Table 1 lists the calibrated model parameters for the soft Bangkok clay.

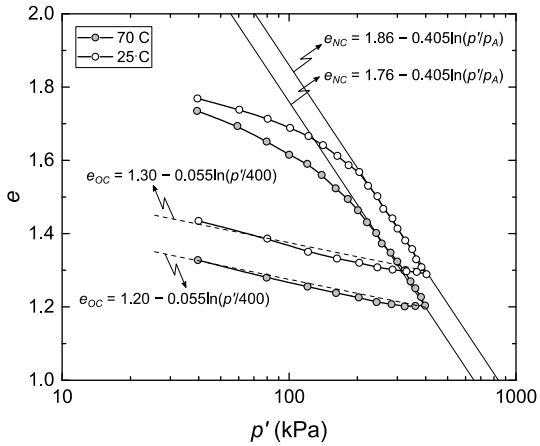

Figure 2 Calibration of the N_{ref}, λ, κ and α (experimental data from Abuel-Naga et al. (2007))

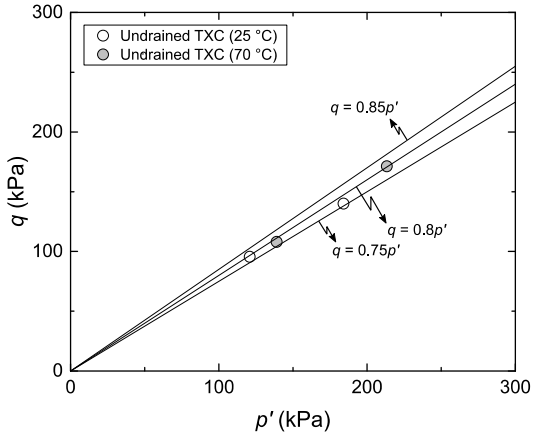

Figure 3. Calibration of the M_c (experimental data from Abuel-Naga et al. (2007))

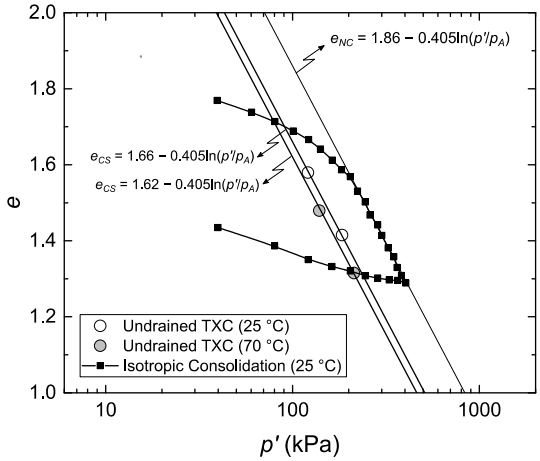

Figure 4. Calibration of the Γ_{ref} and β (experimental data from (Abuel-Naga et al. 2007))

Table 1 Calibrated model parameters for the soft Bangkok clay (Abuel-Naga et al. 2007)

Parameters	Value
N_{25}	1.860
λ	0.405
κ	0.055
ν	0.300
Γ_{25}	1.660
M_c	0.800
α	2.22e−3
β	8.89e−4

4 NUMERICAL SIMULATIONS

Figure 5 illustrates the shape of bounding surfaces with different temperature and same p'_c. As shown in Figure 5, the bounding surface in this study has the greater distortion at higher temperature. When temperature increases, the amount of shift of NCL is greater than the amount of shift of CSL; thus, p'_{cs} locates the nearer to the p'_c with the higher temperature. Temperature does not affect M_c; thus, with the higher p'_{cs}, the apex (= (p'_{cs}, $M_c p'_{cs}$)) of the bounding surface exists at the higher location with the higher temperature.

In this study, to verify the proposed bounding surface, multiple elemental simulations were performed to describe experimental data of undrained triaxial compression tests after isotropic consolidation (CIUTXC) from Abuel-Naga et al. (2007). In the elemental simulations for undrained triaxial compression tests (where no consolidation happens), this study assumed no evolution of p'_c and M; thus, p'_c is fixed and $M = M_c$ during numerical simulation.

Figure 6 and Figure 7 show the experimental data and simulation results of CIUTXC tests for normally consolidated soft Bangkok clay samples under p'_c = 200 kPa when T = 25 °C and 70 °C. Figure 8 and Figure 9 plot the experimental data and simulation results of CIUTXC tests for normally consolidated soft Bangkok clay samples under p'_c = 300 kPa when T = 25 °C and 70 °C. Figure 6 and Figure 8 plot the axial strain versus shear stress q whereas Figure 7 and Figure 9 show the stress paths in the p'-q plane. In all figures, symbols represent experimental data and lines represent simulation results.

In Figure 6 and Figure 8, although there is some disagreement in initial shearing responses, the simulated response agrees closely with the experimental data after axial strain reaches about 4%. This initial difference is closely related to the elastic moduli; more realistic formulation for G and K can improve the model performance.

In Figure 7 and Figure 9, the present model can describe the p'-q responses quite close to the experimental data when T = 25 °C without any evolution rule. When T = 70 °C, initial p'-q responses have difference from the experimental data; however, the model can capture the final destinations (which corresponds to the critical state) of the clay samples precisely.

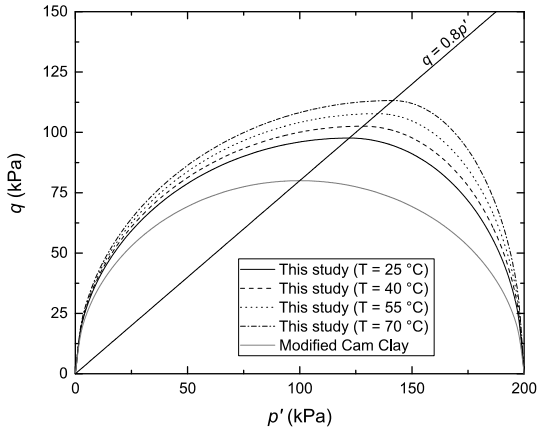

Figure 5. Bounding surfaces for the soft Bangkok clay at different temperature values with the original MCC bounding surface

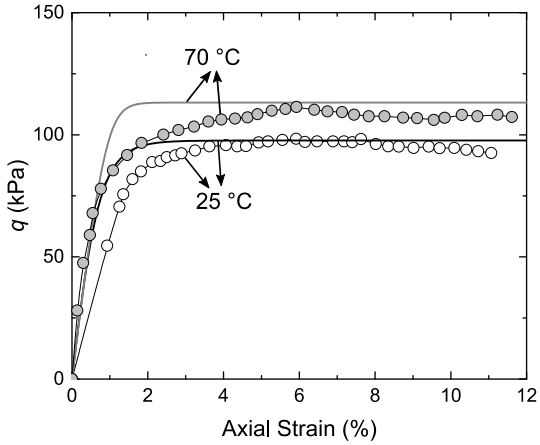

Figure 6 Experimental data and simulation results for the normally consolidated soft Bangkok clay sheared in undrained triaxial compression for various temperature and pre-consolidation pressure p'_c = 200 kPa: axial strain versus shear stress q

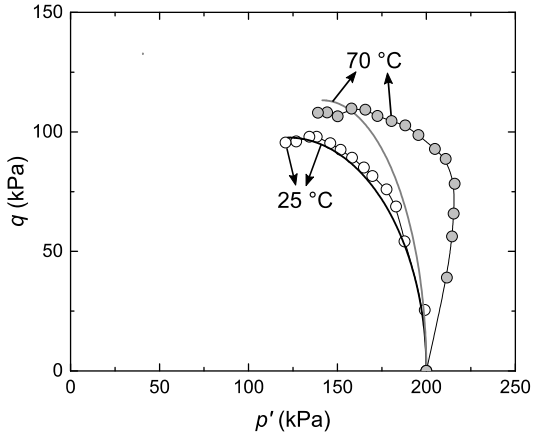

Figure 7 Experimental data and simulation results for the normally consolidated soft Bangkok clay sheared in undrained triaxial compression for various temperature and pre-consolidation pressure p'_c = 200 kPa: mean effective stress p' versus shear stress q

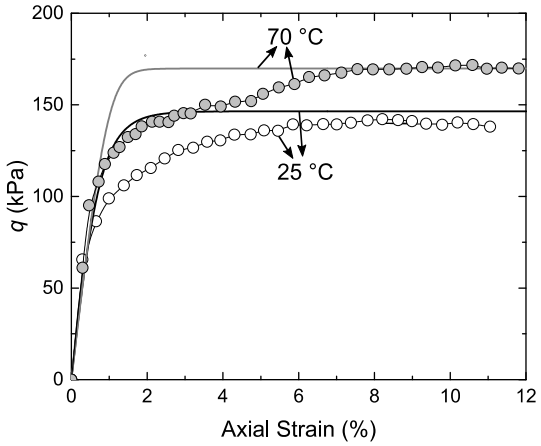

Figure 8 Experimental data and simulation results for the normally consolidated soft Bangkok clay sheared in undrained triaxial compression for various temperature and pre-consolidation pressure p'_c = 300 kPa: axial strain versus shear stress q

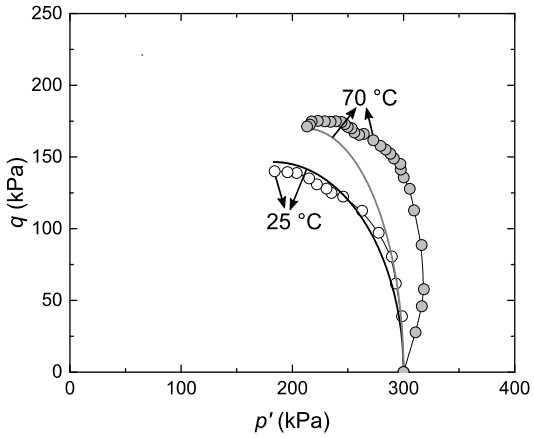

Figure 9 Experimental data and simulation results for the normally consolidated soft Bangkok clay sheared in undrained triaxial compression for various temperature and pre-consolidation pressure p'_c = 300 kPa: mean effective stress p' versus shear stress q

5 SUMMARY AND FUTURE STUDY

This study proposed a new distorted MCC type bounding surface. To describe the ratio between p'_c (which is the right end of the bounding surface in the p'-q plane) and p'_{cs} (which corresponds the apex of the surface) depending on temperature, the bounding surface consists of two parts divided at p' = p'_{cs}. As a result, the shape of bounding surface changes according to temperature.

Total eight model parameters were calibrated for the soft Bangkok clay. Using these parameters, the model can capture the dependency of NCL and CSL on temperature numerically.

Elemental simulations with the proposed model showed the model performance to capture the critical state (which is destination of clay upon shearing) without complex hardening and evolution rules. To improve the model performance, following future researches are planed: 1) adoption of the more realistic elastic moduli for clay, 2) proposal of flow, hardening, and evolution rules, and 3) thermomechanical creep (or secondary compression) and its effects on the bounding surface.

ACKNOWLEDGMENT

The authors gratefully acknowledge the financial support from the National Research Foundation of Korea (NRF) grant funded by the Korea government (No. NRF-2018R1A2B2002869).

REFERENCE

Abuel-Naga, H.M., Bergado, D.T., and Lim, B.F. 2007. Effect of Temperature on Shear Strength and Yielding Behavior of Soft Bangkok Clay. *Soils and Foundations*, **47**(3): 423–436. doi:10.3208/sandf.47.423.

Brochard, L., Honório, T., Vandamme, M., Bornert, M., and Peigney, M. 2017. Nanoscale origin of the thermo-mechanical behavior of clays. *Acta Geotechnica*, **12**(6): 1261–1279. doi:10.1007/s11440-017-0596-3.

Graham, J., Tanaka, N., Crilly, T., and Alfaro, M. 2001. Modified Cam-Clay modelling of temperature effects in clays. *Canadian Geotechnical Journal*, **38**(3): 608–621. doi:10.1139/t00-125.

Hamidi, A., Tourchi, S., and Khazaei, C. 2014. Thermomechanical Constitutive Model for Saturated Clays Based on Critical State Theory. *International Journal of Geomechanics*, **15**(1): 04014038. doi:10.1061/(asce)gm.1943-5622.0000402.

Neaupane, K.M., Nanakorn, P., Sirayapivat, O., and Kanborirak, S. 2005. Effects of temperature on 1-D consolidation characteristics of clayey soil. *In* 16*th International Conference on Soil Mechanics and Geotechnical Engineering*. Osaka, Japan. pp. 417–420. doi:10.3233/978-1-61499-656-9-417.

Plum, R.L., and Esrig, M.I. 1969. Some temperature effects on soil compressibility and pore water pressures. *Highway Research Board Special Report*, **103**(10): 231–242. doi:10.1093/imrn/rnu015.

Sultan, N., Delage, P., and Cui, Y.J. 2002. Temperature effects on the volume change behaviour of Boom clay. *Engineering Geology*, **64**(2–3): 135–145. doi:10.1016/S0013-7952(01)00143-0.

Wang, L.Z., Wang, K.J., and Hong, Y. 2016. Modeling Temperature-Dependent Behavior of Soft Clay. *Journal of Engineering Mechanics*, **142**(8): 04016054. doi:10.1061/ (ASCE)EM.1943-7889.0001108.